

ExoFit: orbital parameters of extra-solar planets from radial velocities

Sreekumar T. Balan^{1,2*} and Ofer Lahav^{1†}

¹*Department of Physics and Astronomy, University College London, Gower Street, London, WC1E 6BT, UK*

²*Astrophysics Group, Cavendish Laboratory, JJ Thomson Avenue, Cambridge, CB3 0HE, UK*

Accepted 2008 December 10. Received 2008 December 9; in original form 2008 May 21

ABSTRACT

Retrieval of orbital parameters of extrasolar planets poses considerable statistical challenges. Due to sparse sampling, measurement errors, parameters degeneracy and modelling limitations there are no unique values of basic parameters such as period and eccentricity. Here we estimate the orbital parameters from radial velocity data in a Bayesian framework by utilising Markov Chain Monte Carlo (MCMC) simulations with the Metropolis-Hastings algorithm. We follow a methodology recently proposed by Gregory and Ford. Our implementation of MCMC is based on the object oriented approach outlined by Graves. We make our resulting code, *ExoFit*, publicly available with this paper. It can search for either one or two planets as illustrated on mock data. As an example we re-analysed the orbital solution of companions to HD 187085 and HD 159868 from the published radial velocity data. We confirm the degeneracy reported for orbital parameters of the companion to HD 187085 and show that a low eccentricity orbit is more probable for this planet. For HD 159868 we obtained slightly different orbital solution and a relatively high ‘noise’ factor indicating the presence of an unaccounted signal in the radial velocity data. *ExoFit* is designed in such a way that it can be extended for a variety of probability models, including different Bayesian priors.

Key words: stars:planetary systems - stars: individual: HD 187085, HD 159868 - techniques: radial velocities - methods: data analysis - methods: statistical - methods: numerical.

1 INTRODUCTION

The study of extra-solar planets is of great importance because it helps us to understand the origin and evolution of the Solar System. The information gained from analysing new stellar systems serves as a sign post towards finding possible life forms outside our Solar System. The first 200 or so detected extra-solar planets has been discovered using the radial velocity method. Other detection methods include astrometric method, transit photometry, gravitational micro-lensing and direct imaging. Astrometric method look for the periodic shifts in the position of star and transit method measures the attenuation of star light caused by the passage of the planet across the star. Gravitational micro-lensing utilises the amplification of light rays from the background object by an intervening massive object. In a number of cases, existence of the planet has been confirmed by more than one method. The number of multi-planet systems

discovered has also increased during the past few years due to the improved precision of radial velocity measurements.

In this article, we are concerned with the extraction of orbital parameters from observed radial velocity data. A survey of the literature in this field indicates that orbital parameters and their uncertainties were traditionally obtained by a two step method. Searching for periodicity in the radial velocity data using a Lomb-Scargle (Lomb 1976; Scargle 1982) periodogram to fix the orbital period and then estimating other parameters by Levenberg-Marquardt (Levenberg 1944; Marquardt 1963) minimisation. Recently, Bayesian methods have been applied (Gregory 2005a; Ford 2005; Ford & Gregory 2007) to find out the best fit orbital parameters and these studies suggest that Bayesian techniques have considerable advantages over the traditional methods; for e.g when the data does not cover a single orbital phase of the planet. In this work we analyse the radial velocity data from a Bayesian point of view and extract the orbital parameters and corresponding uncertainties using Markov Chain

* E-mail: st452@mrao.cam.ac.uk

† E-mail: lahav@star.ucl.ac.uk

Monte Carlo (MCMC) simulations. We make our code, *ExoFit*, and a detailed documentation available on-line¹.

The outline of the paper is as follows. In Section 2 we summarise the modelling of radial velocities. In Section 3 we discuss the Bayesian approach to the problem. In Section 4 we present the MCMC implementation and the *ExoFit* software package. *ExoFit* is then applied to mock and observed data in Sections 5 and 6 respectively. The results are discussed in Section 7.

2 MODELLING OF RADIAL VELOCITY

2.1 Doppler Spectrography

Planets are many times fainter than their host stars because they shine only by reflecting the star light. This makes their direct imaging extremely difficult. However, the gravitational pull of the planet makes the star wobble and this produces measurable periodic shifts in the apparent speed of the parent star. The motion of the star around the centre of mass causes the observed spectrum of the star to be Doppler shifted according to its radial velocity, i.e. the velocity along the line of sight of the observer. This is measured over a course of time to obtain the radial velocity data along with the measurement uncertainties.

2.2 Radial Velocity of Star

A single planet model is assumed here to analyse the radial velocity data. The radial velocity of a star can be written as (Murray & Dermott 2000; Ohta et al. 2005)

$$\begin{aligned} v_i &= V - K(\sin(f_i + \varpi) + e \sin \varpi) \\ K &= \frac{m_p}{m_s + m_p} \frac{na \sin i}{\sqrt{1 - e^2}} \end{aligned} \quad (1)$$

where v_i is the i th radial velocity entry corresponding to time coordinate t_i and,

V = the systematic velocity of the system,

m_p = the mass of the planet,

m_s = the mass of the star,

$n = \frac{2\pi}{T}$ the mean motion and T is orbital period of planet,

a = the length of the semi-major axis of the planet,

i = the inclination of the orbital plane with the ecliptic,

e = the eccentricity of the planet,

f_i = the true anomaly at time t_i and

ϖ = the longitude of periastron.

The radial velocity depends on time via the true anomaly f_i . The full formalism and comparison with a common approximation is discussed in the User's Guide to *ExoFit*.

2.3 Radial velocity data

According to (<http://exoplanet.eu>) eighteen different radial velocity search programmes are looking for extrasolar planets. Majority of the contributions come from Keck, Lick and Anglo-Australian observatories (the California & Carnegie and Anglo-Australian planet searches) and searches based

at l'Observatoire de Haute Provence and La Silla Observatory (the Geneva extrasolar planet search). Radial velocity data for a star consists of time of observation t_i , measured radial velocity v_i and uncertainty associated with each measurement e_i . These uncertainties are a characteristic of the instruments used for measurements. The precision of these instruments have improved from the order of 10ms^{-1} in 1994 to order of 1ms^{-1} (Butler et al 2006; Pepe et al. 2004) at present.² This is extremely significant for finding low mass companions as well as planets with large a s.

3 BAYESIAN RETRIEVAL OF ORBITAL PARAMETERS

3.1 Introduction

The extraction of orbital parameters from the radial velocity data poses considerable statistical challenges. Earlier in this article we mentioned the traditional two step method that is generally used to retrieve orbital parameters. Studies by Cumming (2004) and Cumming et al. (1999) have identified two cases where these methods become inefficient in accurately characterising the orbital elements:

- (i) When the orbital period is extremely short and the eccentricity is high.
- (ii) When the duration of observation does not span at least a single orbital phase.

Incomplete radial velocity data gives rise to a multitude of orbital solutions which is referred to as parameter degeneracy. Since the transit probability of the planet increases for short periods, the orbital parameters predicted by the periodogram method can be verified, in some cases, with the help of transit photometry. Higher eccentricities make the radial velocity curve less sinusoidal. O'Toole et al. (2007) makes use of a 2DKLS periodogram to incorporate the effect of eccentricity of the orbits while searching for orbital periods. Recently Bayesian techniques have been employed by Gregory (2005a), Ford (2005) and Ford & Gregory (2007) to retrieve the orbital parameters of extra-solar planets. The results show that Bayesian methods tackle the difficulties associated with the traditional methods efficiently and transparently. We emphasise that the relative merit of different methods depends on the quality of the data. Broadly speaking the choice of prior distribution may change the inference (posterior distribution) significantly when the quality of data is poor.

3.2 The Bayesian method

The starting point of any Bayesian analysis is Bayes' theorem (Bayes 1763). Let $\mathbf{y} = (y_1, \dots, y_i, \dots, y_n)$ be a vector of n observations whose probability distribution $p(\mathbf{y}|\boldsymbol{\theta}, H)$ is conditional on k parameters $\boldsymbol{\theta} = (\theta_1, \dots, \theta_i, \dots, \theta_k)$, where H represents the background information or the hypothesis by which the probability statements are made. Suppose that

¹ <http://www.star.ucl.ac.uk/~lahav/exofit.html>

² The measurement method and its uncertainties are discussed in the corresponding planet discovery papers.

the parameter θ has the probability distribution $p(\theta|H)$. Then, Bayes' theorem says

$$p(\theta|\mathbf{y}, H) = \frac{p(\mathbf{y}|\theta, H)p(\theta|H)}{p(\mathbf{y}|H)}. \quad (2)$$

For a continuous θ we can write

$$p(\mathbf{y}|H) = \int p(\mathbf{y}|\theta, H)p(\theta|H) d\theta, \quad (3)$$

which is constant for given \mathbf{y} and a probability distribution $p(\theta|H)$. Then Equation [2] can be rewritten as

$$p(\theta|\mathbf{y}, H) = C p(\mathbf{y}|\theta, H)p(\theta|H). \quad (4)$$

In the above equation $p(\theta|H)$ is called *prior distribution* of θ since it conveys our knowledge about θ before the data has been observed. Correspondingly, $p(\theta|\mathbf{y}, H)$ is known as the *posterior distribution* of θ given \mathbf{y} . The factor C is a normalising constant which ensures that the posterior distribution integrates to one. We call $p(\mathbf{y}|\theta, H)$ the likelihood function of θ since $p(\mathbf{y}|\theta, H)$ can be considered as a function of θ instead of \mathbf{y} . Then,

$$p(\theta|\mathbf{y}, H) \propto p(\mathbf{y}|\theta, H)p(\theta|H). \quad (5)$$

Statistical inferences regarding θ are derived from the posterior distribution of θ . The posterior distribution encapsulates all information about unknown quantities θ following the observation of the data \mathbf{y} . The principal steps in the Bayesian method can be involve the Likelihood $p(\mathbf{y}|\theta, H)$, the prior $p(\theta|H)$, the posterior $p(\theta|\mathbf{y}, H)$, and the resulting inference, e.g. O'Hagan & Forster (2004).

3.3 Likelihood function

Let d_i represent the measured radial velocity data for the i th instant of time t_i . Observed radial velocity data can be modelled by the equation (Gregory 2005a)

$$d_i = \nu_i + \epsilon_i + \delta, \quad (6)$$

where ν_i is the true radial velocity of the star and ϵ_i is the uncertainty component arising from accountable but unequal measurement errors which are assumed to be normally distributed. The term δ explains any unknown measurement errors. There can be multiple reasons for the presence of this uncertainty component (Butler et al 2006). For example this could be the result of another planet in the system or caused by the intrinsic anomalies in the star spectrum due to the irregularities on the surface of the star (Pepe et al. 2004; Mayor et al. 2003; Bouchy et al. 2005). Thus any noise component that cannot be modelled is described by the term δ . The probability distribution of δ is chosen to be a Gaussian distribution with finite variance s^2 . Therefore the combination of uncertainties $\epsilon_i + \delta$ has a Gaussian distribution with a variance equal to $\sigma_i^2 + s^2$.

The true radial velocity ν_i is modelled by the equation (2). Thus the radial velocity v_i predicted by the mathematical model at an instant t_i is

$$v_i = V - K (\sin(fi + \varpi) + e \sin \varpi).$$

Six model parameters namely $T, K, V, e, w,$ and χ , as defined in the section (2.2) are used to fit the above equation onto a given radial velocity data.

Each error term ϵ_i in equation (6) is independent. Since

Table 1. The assumed prior distribution of various parameters and their boundaries. It is similar to choice of priors given by Ford & Gregory (2007), except for the prior distribution of K .

Para.	Prior	Mathematical Form	Min	Max
$T(days)$	Jeffreys	$\frac{1}{T \ln \left(\frac{T_{max}}{T_{min}} \right)}$	0.2	15000
$K(ms^{-1})$	Mod. Jeffreys	$\frac{(K+K_0)^{-1}}{\ln \left(\frac{K_0+K_{max}}{K_0} \right)}$	0.0	2000
$V(ms^{-1})$	Uniform	$\frac{1}{V_{max}-V_{min}}$	-2000	2000
e	Uniform	1	0	1
ϖ	Uniform	$\frac{1}{2\pi}$	0	2π
χ	Uniform	1	0	1
$s(ms^{-1})$	Mod. Jeffreys	$\frac{(s+s_0)^{-1}}{\ln \left(\frac{s_0+s_{max}}{s_0} \right)}$	0	2000

they are assumed to follow a Gaussian distribution, the likelihood function is product of N Gaussians (Gregory 2005b,a) where N is the number of observations. Thus

$$p(\mathbf{y}|\theta) = A \exp \left[- \sum_{i=1}^N \frac{(d_i - v_i)^2}{2(\sigma_i^2 + s^2)} \right], \quad (7)$$

where

$$A = (2\pi)^{-N/2} \left[\prod_{i=1}^N (\sigma_i^2 + s^2)^{-1/2} \right]. \quad (8)$$

and s becomes the seventh parameter in our probability model.

3.4 Choice of Priors

The choice of priors is extremely important in the Bayesian analysis as senseless choice of priors can produce to misleading results. Physical and geometric conditions govern the selection of prior distributions for most of the parameters. Since $\theta = (T, K, V, e, \varpi, \chi, s)$ the prior distribution in our problem can be written as

$$p(\theta|H) = p(T|H)p(K|H)p(V|H)p(e|H)p(\varpi|H)p(\chi|H)p(s|H), \quad (9)$$

on the assumption that they are independent. We will discuss how the above conditions are met for our choice of prior for each parameter in the next few sections.

We follow the choice of priors as given by Ford & Gregory (2007), as summarized in Table 1. Obviously, part of the Bayesian framework is the ability to change priors and to check the sensitivity of the results to them. Our *ExoFit* package allows this freedom.

3.5 Posterior Distribution

Posterior distribution is obtained by applying the Bayes' theorem given by the equation (4). Useful and interesting features of the posterior distribution should be identified before making summary statements. For example, the posterior distribution may be unimodal but asymmetric or it can be multi-modal with many probability peaks. Any summary statistic(e.g. mean, median and mode) can be expressed in terms of posterior expectations of θ (Gilks et al. 1996; Berger 1980).

4 MCMC IMPLEMENTATION

4.1 The MCMC approach

Difficulty in evaluating the multi-dimensional integrals is an inherent inability of any Bayesian formulation. Many techniques have been developed in the last 25 years to deal with this problem. Simulation methods dominate this area and several computational algorithms were developed to numerically integrate the posterior distribution in order to find out the marginal distributions of each parameter. According to Berg (2004) the abundance of computational power has produced a paradigm shift with respect to statistics: Computationally intensive but conceptually simple methods are preferred. Markov Chain Monte Carlo (MCMC) method is one of the most commonly used methods for simulating complex probability distributions³. Our code is based on the concepts outlined by Graves (2007). The emphasis is on the extensibility of the code to accommodate different probability models to a certain extent.

Bayesian MCMC methods have gained popularity in various areas of astrophysics, for example in multi-parameter estimation from cosmological data sets (e.g. CosmoMC; Lewis & Bridle (2002)). We emphasise that the two ingredients, the Bayesian approach and the MCMC tool, are distinct and not necessarily related. One may apply MCMC to a multi-parameter likelihood analysis (i.e. without priors—equivalent to a Bayesian method for uniform priors). On the other hand one may work out a full Bayesian method (with complicated priors) using a grid-based maximisation procedure, without the need for MCMC. Having said that, the combination of the Bayesian and MCMC methods is a very powerful way to tackle our problem.

From a Bayesian point of view analysis of statistical problems requires an efficient tool for simulating posterior densities and MCMC methods are ideally suited for this purpose. In general, one must consider planet-planet interaction while modelling radial velocity of a star. In typical systems the radial velocity of an n -planet model can be approximated as a linear combination of n single planet radial velocities. With the present version of *ExoFit* it is possible to search for either one or two planets.

4.2 The *ExoFit* software package

ExoFit is a step towards achieving the goals mentioned above. It should be considered as a platform to develop MCMC based methods for estimating orbital parameters of a generalised multi-planet model. Object oriented design of *ExoFit* makes it extremely well suited for extending the analysis to multi-planet systems with prior constraints on several orbital parameters such as eccentricity and length of semi-major axis. Following Graves (2007), our implementation MCMC consists of Data, State, Bond and Update. They are referred to as objects in object oriented analysis. *data* handles the input data into the MCMC analysis. A *state* consists of a set of parameters whose posterior distribution is sought. The parameter values at a particular in-

stant defines the *state* of Markov Chain in the analysis. The parameters in a particular *state* are connected to each other by a *bond*. It consists of prior densities and likelihood. For each state there corresponds a bond strength which is equal to $prior \times likelihood$. In other words it is the posterior density without the normalisation constant in Bayes' theorem. An *update* selects the parameters that should be updated at particular iteration. New values for the parameters are proposed according to the *update* defined and the new *bond* strength is then calculated for the proposed state. The new state is accepted or rejected according to Metropolis-Hastings method.

The central concept of this approach is that, the MCMC engine remains the same and need not be re-implemented whenever the probability model gets changed. We also take advantage of the commonalities among the different components of MCMC. Our implementation works for variety of prior distributions (*Bonds*) and *Update* methods. The only component that requires to be changed is the likelihood function.

Convergence is an important aspect of any MCMC method and the choice of proposal distribution is absolutely crucial for achieving convergence of the chain. Choosing an effective proposal distribution is very difficult in many cases. *ExoFit* employs an adaptive Metropolis algorithm described by Haario et al. (1999) to fine tune the proposal distribution step sizes.

5 APPLICATION TO MOCK DATA

We used simulated data sets to test the accuracy of the orbital parameters extracted by *ExoFit*. The output of *ExoFit* is analysed with the help of the R statistical environment⁴ which is freely available. A number of packages are available in R for checking the convergence of Markov Chains and creating the histograms and density plots of posterior distribution of parameters.

5.1 1-planet data with 1-planet fit

In this The first set of radial velocity entries as shown in Table 2 (columns 1, 2 and 3) is created using a single planet model (equation (2)) and adding a Gaussian noise. Table 3 shows the input parameters used to create the data set and the parameters obtained with *ExoFit* for a single planet search. Three posterior summary statistics are compared in Table 3; where column 2 gives the assumed input values, column 3 contains the mean values of MCMC samples for each parameter along with the sample standard deviation, column 4 shows the median values with 75% and 25% quantiles. We used Hyndman (1996)'s method to calculate *Highest Density Regions* (HDRs) of the posterior distribution. Column 5 contains posterior modes (maximum a posteriori) and associated 68.3% credible regions. The difference between actual radial velocity curve and the radial velocity curve for the parameters obtained from *ExoFit* is shown in the Fig. 1. We also plot the deviation of the radial velocities from the actual one for each of these orbital solutions in

³ A general form this method given by *Metropolis-Hastings* (Metropolis et al. 1953; Hastings 1970) algorithm is explained in *ExoFit User Guide*.

⁴ <http://www.r-project.org/>

Table 2. Column 2 shows the simulated radial velocities obtained from a single planet model (Table 3) using equation (2). A Gaussian noise with $\mu = 0.0ms^{-1}$ and $\sigma = 2.0ms^{-1}$ has been added to each radial velocity term. Columns 3 is obtained by adding the radial velocity from a second planet (see Table 3) to each term in column 2, thus creating a mock radial velocity data for a two planet system. The measurement uncertainties (Gaussian distribution with $\mu = 2.0ms^{-1}$ and $\sigma = 0.5ms^{-1}$) are shown in columns 4 and 5.

<i>JD</i> (-2451000)	<i>RV</i> (<i>ms</i> ⁻¹)	<i>Error</i> (<i>ms</i> ⁻¹)	<i>RV</i> (<i>ms</i> ⁻¹)	<i>Error</i> (<i>ms</i> ⁻¹)
1-planet		2-planets		
1400.15200	-17.90	2.1	-25.30	2.1
1413.87749	-18.50	2.8	-18.20	2.8
1434.46573	-30.00	1.4	-22.50	1.4
1455.05396	-33.00	2.0	-26.20	2.0
1489.36769	-41.10	2.1	-52.70	2.1
1496.23043	-41.30	2.4	-50.80	2.4
1503.09318	-45.50	1.7	-51.20	1.7
1564.85788	-47.60	1.7	-45.30	1.7
1571.72063	-44.20	2.0	-46.80	2.0
1585.44612	-39.40	1.6	-50.70	1.6
1592.30886	-33.60	1.9	-44.70	1.9
1612.89710	-14.50	1.9	-14.70	1.9
1619.75984	-6.17	1.9	-3.07	1.9
1654.07357	38.20	2.4	45.30	2.4
1688.38729	61.90	1.6	50.30	1.6
1695.25004	64.90	1.7	54.90	1.7
1715.83827	74.00	2.9	75.30	2.9
1722.70102	73.70	2.7	78.00	2.7
1736.42651	70.20	1.8	78.00	1.8
1743.28925	72.70	2.6	81.10	2.6
1770.74024	67.30	2.3	65.50	2.3
1777.60298	65.10	2.0	57.80	2.0
1784.46573	66.20	2.7	55.20	2.7
1798.19122	61.90	2.4	53.40	2.4
1811.91671	56.70	1.9	56.00	1.9
1818.77945	56.20	2.2	58.80	2.2
1832.50494	51.00	1.7	58.20	1.7
1901.13239	32.80	1.6	25.90	1.6
1907.99514	32.40	2.0	29.60	2.0
1921.72063	29.80	2.2	33.70	2.2
1928.58337	33.90	3.7	40.10	3.7
1935.44612	29.10	2.9	36.80	2.9
1962.89710	19.00	2.2	22.40	2.2
1969.75984	17.40	2.2	16.30	2.2

Table 3. A comparison between input parameters to the mock data for 1 and 2 planets and the parameters extracted with *ExoFit* 1-planet model. Columns 3, 4 and 5 show the posterior mean (and standard deviation), median (and 25% and 75% quantiles) and the maximum a posteriori, i.e. the posterior mode (and 68.3% highest density regions) obtained by the application of *ExoFit* 1-planet model to the single planet data from Table 2. Column 6 shows the orbital parameters of the second planet used to simulate the data for the two planet system (columns 4 and 5 in Table 2). Summary statistics of the posterior distribution generated with *ExoFit* 1-planet model for this 2-planet data is shown in columns 7, 8 and 9. Note the difference between the noise factors extracted with *ExoFit* from the single planet data and the 2-planet data. Thus the noise factor *s* serves as an indicator for a possible embedded signal in the radial velocity data apart from the random Gaussian errors.

Parameter	Planet 1	<i>ExoFit</i> Mean	<i>ExoFit</i> Median	<i>ExoFit</i> Mode	Planet 2	<i>ExoFit</i> Mean	<i>ExoFit</i> Median	<i>ExoFit</i> Mode
<i>V</i> (<i>ms</i> ⁻¹)	12.0	11.91 ± 0.44	11.91 ^{+0.30} _{-0.30}	11.91 ^{+0.44} _{-0.45}		11.50 ± 1.60	11.55 ^{+1.00} _{-1.05}	11.69 ^{+1.43} _{-1.64}
<i>T</i> (<i>days</i>)	700.00	704.85 ± 12.91	704.24 ^{+9.03} _{-8.36}	702.79 ^{+13.62} _{-11.67}	100.0	719.11 ± 53.06	711.23 ^{+33.62} _{-27.52}	704.95 ^{+44.76} _{-43.50}
<i>K</i> (<i>ms</i> ⁻¹)	60.00	60.39 ± 0.56	60.39 ^{+0.38} _{-0.38}	60.37 ^{+0.58} _{-0.54}	10.0	62.52 ± 2.25	62.51 ^{+1.44} _{-1.46}	62.48 ^{+2.19} _{-2.20}
<i>e</i>	0.38	0.38 ± 0.03	0.38 ^{+0.01} _{-0.01}	0.38 ^{+0.01} _{-0.02}	0.18	0.40 ± 0.04	0.40 ^{+0.03} _{-0.03}	0.40 ^{+0.04} _{0.04}
ϖ	3.10	3.09 ± 0.03	3.09 ^{+0.02} _{-0.02}	3.04 ^{+0.02} _{-0.03}	1.10	2.96 ± 0.11	2.96 ^{+0.07} _{-0.07}	2.96 ^{+0.11} _{-0.11}
χ	0.67	0.67 ± 0.00	0.67 ^{+0.00} _{-0.01}	0.67 ^{+0.00} _{-0.01}	0.17	0.69 ± 0.01	0.69 ^{+0.01} _{-0.01}	0.68 ^{+0.01} _{-0.01}
<i>s</i>		0.4276 ± 0.35	0.34 ^{+0.27} _{-0.19}	0.09 ^{+0.43} _{-0.09}		7.49 ± 1.14	7.36 ^{+0.80} _{-0.66}	7.12 ^{+0.93} _{-0.93}

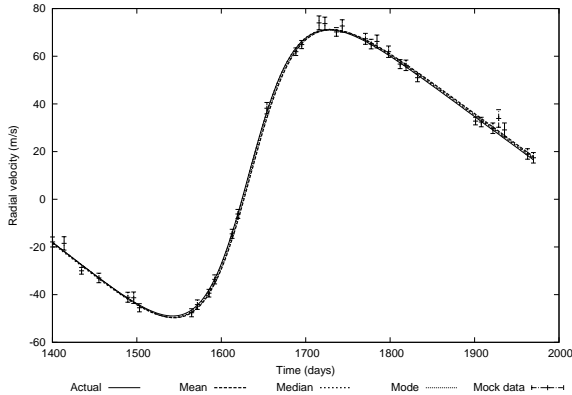


Figure 1. Radial velocity curves created with mean, median and mode of the posterior distribution of parameters. The radial velocity curve for actual input parameters with the simulated data is also shown.

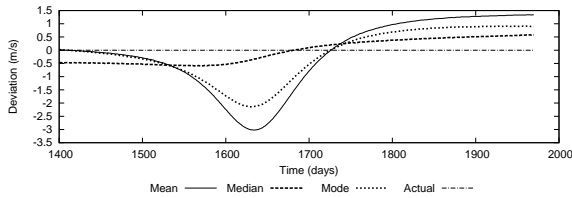


Figure 2. Deviation from the actual radial velocities of the simulated data for 3 different summary statistics shown in Table 3. Note the differences are no more than $3ms^{-1}$.

Fig. 2. We note the deviations between the estimators are smaller than $3ms^{-1}$. The noise factor $s \approx 0.4$ is less than the measurement uncertainties, implying the assumed radial velocity model is “good” and there is no sign of an additional signal present in the data.

5.2 2-planet data with 1-planet fit

A second set of radial velocity entries as shown in column 4 of Table 2 has been created by adding the radial velocity from a second planet with orbital parameters as shown in Table 3 to the radial velocity data of the single planet model in column 2 of Table 2. The results from the application of *ExoFit* to this simulated data is shown in columns 7, 8 and 9 of Table 3. Noise factor $s \approx 7ms^{-1}$ in this case is clearly higher than the measurement uncertainties, indicating the presence of a signal unaccounted for in the radial velocity model. Note that the noise factor obtained in the previous case was only $\approx 0.4ms^{-1}$. Fig. 3 shows the radial velocity curve for the median values of the posterior distribution of orbital parameters from *ExoFit* along with the actual radial velocity plot for the 2-planet model.

5.3 A 2-planet fit to 2-planet mock data

ExoFit has an option to search for two planets in the radial velocity data. We choose the probability model to be similar to that of the single planet model explained in Section 3.3. The observed radial velocity data is again modelled by the equation 6. The radial velocity v_i predicted by the

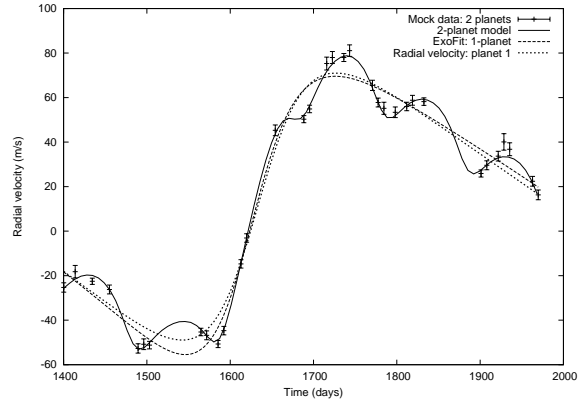


Figure 3. The radial velocity curve for two planet model with orbital parameters of the planets from Table 3 along with the radial velocity plot created with median values of parameters obtained by *ExoFit* (median values) and the actual radial velocity.

Table 4. The assumed prior distribution of orbital parameters and their boundaries for a 2-planet model. The boundaries for K_2 can be made smaller in order to speed up the convergence of the Markov Chain.

Para.	Prior	Mathematical Form	Min	Max
$V(ms^{-1})$	Uniform	$\frac{1}{V_{max} - V_{min}}$	-2000	2000
$T_1(days)$	Jeffreys	$T_1 \ln \left(\frac{T_1 max}{T_1 min} \right)$	0.2	15000
$K_1(ms^{-1})$	Mod. Jeffreys	$\frac{(K_1 + K_1 0)^{-1}}{\ln \left(\frac{K_1 0 + K_1 max}{K_1 0} \right)}$	0.0	2000
e_1	Uniform	1	0	1
ϖ_1	Uniform	$\frac{1}{2\pi}$	0	2π
χ_1	Uniform	1	0	1
$T_2(days)$	Jeffreys	$T_2 \ln \left(\frac{T_2 max}{T_2 min} \right)$	0.2	15000
$K_2(ms^{-1})$	Mod. Jeffreys	$\frac{(K_2 + K_2 0)^{-1}}{\ln \left(\frac{K_2 0 + K_2 max}{K_2 0} \right)}$	0.0	2000
e_2	Uniform	1	0	1
ϖ_2	Uniform	$\frac{1}{2\pi}$	0	2π
χ_2	Uniform	1	0	1
$s(ms^{-1})$	Mod. Jeffreys	$\frac{(s+s_0)^{-1}}{\ln \left(\frac{s_0 + s max}{s_0} \right)}$	0	2000

mathematical model at an instant t_i is given by

$$v_i = V - \left(K_1 (\sin(f_{i1} + \varpi_1) + e_1 \sin \varpi_1) + K_2 (\sin(f_{i2} + \varpi_2) + e_2 \sin \varpi_2) \right). \quad (10)$$

11 parameters $\{V, T_1, K_1, e_1, \varpi_1, \chi_1, T_2, K_2, e_2, \varpi_2, \chi_2\}$ ⁵, as defined in the Section 2.2 are used to fit the above equation onto the radial velocity data. The likelihood function is again given by equations 7 and 8 respectively, and s becomes the 12th parameter in our probability model. The choice of prior distributions for each of these parameters is given in Table 4.

We apply the *ExoFit* to the 2-planet mock radial velocity data given in Table 2 (column 4). A comparison of actual orbital parameters with the ones extracted with *ExoFit* is given in Table 5.3. Fig 4 shows the actual radial velocity curve and the one created with the median values of the posterior distribution of orbital parameters obtained from

⁵ Subscripts 1 and 2 indicate planets 1 and 2 respectively.

Table 5. A comparison of actual values of orbital parameters used to create the mock radial velocity data for the 2-planet system (Columns 4 and 5 in Table 2) and the summary of the posterior distribution of orbital parameters extracted with *ExoFit* 2-planet model. Column 3, 4 and 5 shows posterior mean (and standard deviation), median (and 25% and 75% quantiles) and the maximum a posteriori, i.e. posterior mode (and 68.3% highest density regions) respectively.

Parameter	Actual	<i>ExoFit</i> Mean	<i>ExoFit</i> Median	<i>ExoFit</i> Mode
$V(m s^{-1})$	12.0	11.80 ± 0.52	$11.80^{+0.33}_{-0.35}$	$11.87^{+0.44}_{-0.58}$
$T_1(days)$	700.0	709.06 ± 15.03	$708.25^{+10.32}_{-9.68}$	$708.03^{+14.04}_{-15.36}$
$K_1(m s^{-1})$	60.0	60.34 ± 0.62	$60.33^{+0.41}_{-0.41}$	$60.33^{+0.59}_{-0.64}$
e_1	0.38	0.38 ± 0.01	$0.38^{+0.01}_{-0.0}$	$0.38^{+0.01}_{-0.01}$
ϖ_1	3.10	3.10 ± 0.04	$3.10^{+0.02}_{-0.02}$	$3.11^{+0.03}_{-0.04}$
χ_1	0.67	0.67 ± 0.00	$0.67^{+0.00}_{-0.01}$	$0.67^{+0.00}_{-0.00}$
$T_2(days)$	100.0	100.44 ± 0.53	$100.45^{+0.35}_{-0.36}$	$100.43^{+0.54}_{-0.52}$
$K_2(m s^{-1})$	10.0	10.19 ± 0.62	$10.18^{+0.38}_{-0.41}$	$10.14^{+0.65}_{-0.58}$
e_2	0.18	0.19 ± 0.05	$0.19^{+0.03}_{-0.03}$	$0.20^{+0.05}_{-0.05}$
ϖ_2	1.10	1.27 ± 0.36	$1.28^{+0.23}_{-0.24}$	$1.29^{+0.38}_{-0.38}$
χ_2	0, 17	0.15 ± 0.05	$0.15^{+0.03}_{-0.03}$	$0.15^{+0.05}_{-0.05}$
s		0.50 ± 0.41	$0.40^{+0.33}_{-0.22}$	$0.15^{+0.05}_{-0.05}$

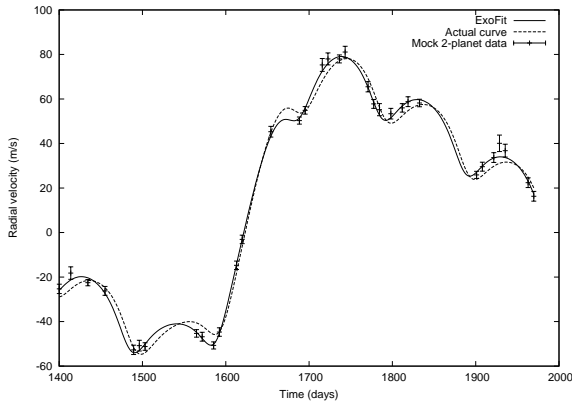


Figure 4. A comparison of the actual 2-planet radial velocity curve and the one obtained with *ExoFit* (median values).

*ExoFit*⁶. Note that the noise factor s is now $\approx 0.4 m s^{-1}$ compared to $s \approx 7 m s^{-1}$ in the single planet model. The density plots are shown in Fig 5.

Constraining the longitude of periastron ϖ becomes increasingly difficult when the eccentricity of planetary system approaches zero. Ford (2006) suggests that, the efficiency of MCMC sampler in this situation can be increased by adopting a new parametrisation with $e \sin \varpi$ and $e \cos \varpi$. For discussions about further improvements in parametrisation, choice of priors and proposal distributions for MCMC, see

⁶ We caution that, using median values for orbital parameters with skewed marginal posterior distributions can lead to models that very poor.

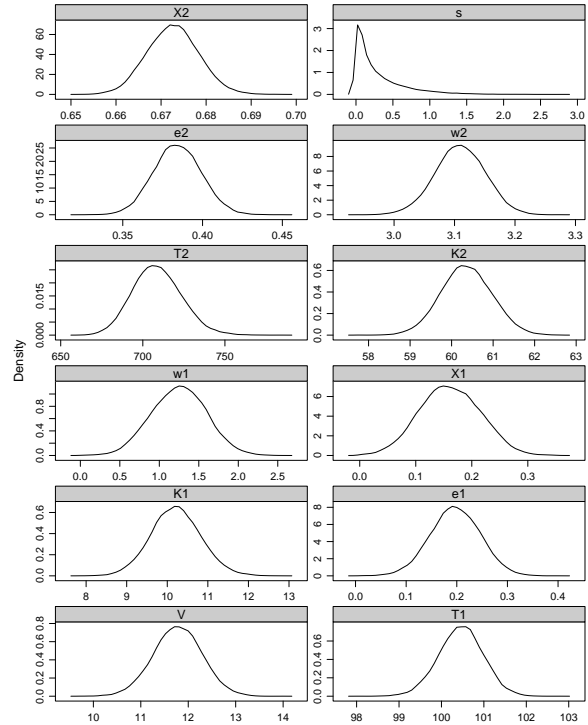


Figure 5. Posterior density of 12 orbital parameters of the 2-planet model obtained from *ExoFit*.

Ford (2006). These considerations will be implemented in the future version of *ExoFit*.

6 APPLICATION TO OBSERVED DATA

In this section we apply *ExoFit* to published radial velocity data. We choose data sets in which the measurement noise is relatively high and the entries are poorly sampled. The following examples shows that *ExoFit* does a good job in estimating the posterior distribution orbital parameters.

6.1 The companion to HD 187085

Detection of a planet orbiting HD 187085 was announced in 2006 with 40 epoch of radial velocity measurements between 1998 November and 2005 October (Jones et al. 2006). It has reported that although an orbital solution of period 986 days and eccentricity 0.47 gave the best fit, a solution with low eccentricity also produced similar fit to the observed data. Application of *ExoFit* revealed the posterior density distribution orbital parameters as shown in Fig. 6. The MCMC values with iterations are shown in the user's manual. It is evident from Fig. 6 that the posterior density of eccentricity is a heavily skewed. The joint probability distributing of orbital period and eccentricity is shown in Fig. 7 with two dimensional HDRs. From these plots it is reasonable to conclude that the data clearly favours a low eccentricity orbit.

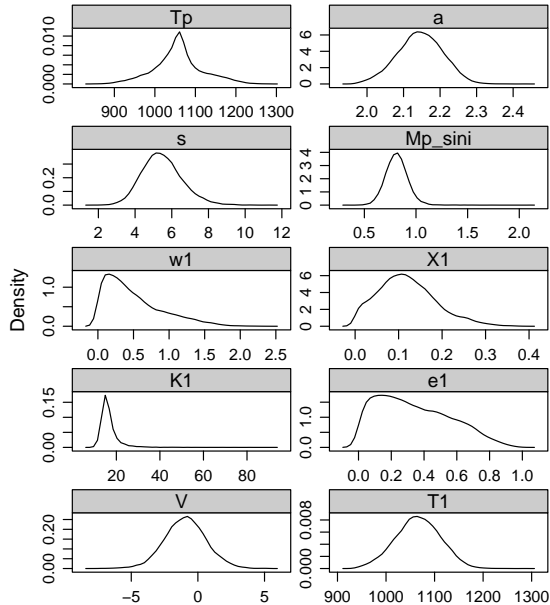


Figure 6. Posterior distribution of orbital parameters of the companion to HD 187085. These plots were created with R from the output of *ExoFit*.

Table 6 shows the summary statistics of the posterior distribution of orbital parameters of HD 187085 along with the published results. The eccentricity is $e = 0.33, 0.30, 0.11$ from the mean, median and mode respectively, compared with the published estimate $e = 0.47$.⁷ Keplerian orbital solutions for HD 187085 from Table 6 shown in Fig. 8.

How sensitive are the results to the assumed priors? In Table 7 we show results based on 10 trial runs of for Gregory’s priors (Table 1) and for Top Hat priors, i.e. uniform between the same lower and upper values as in Gregory’s priors. This indicates the data and assumed model are ‘good’. The role of priors would be more dramatic in the case of poor data.

6.2 The companion to HD 159868

Orbital parameters of a planet orbiting HD 159868 from 28 radial velocity measurements was reported on 2007 by O’Toole et al. (2007). They employed a two-dimensional periodogram to search for the optimum orbital period and the eccentricity for the orbit. The posterior distribution of parameters are shown in Fig. 9 and since they are nearly symmetric, we choose median of the distribution as the point

⁷ For a posterior distribution that is approximately Gaussian (e.g., parameter T), estimates like mean, median and mode will yield nearly the same values. However, when the posterior density is not Gaussian and exhibit skewness (e.g., parameter e) mean, median and mode will differ significantly. Since this is the case for parameter e , posterior median and mode will be a better estimate than posterior mean. If the posterior distribution has more than one peak, posterior modes provide ideal summary of the distribution.

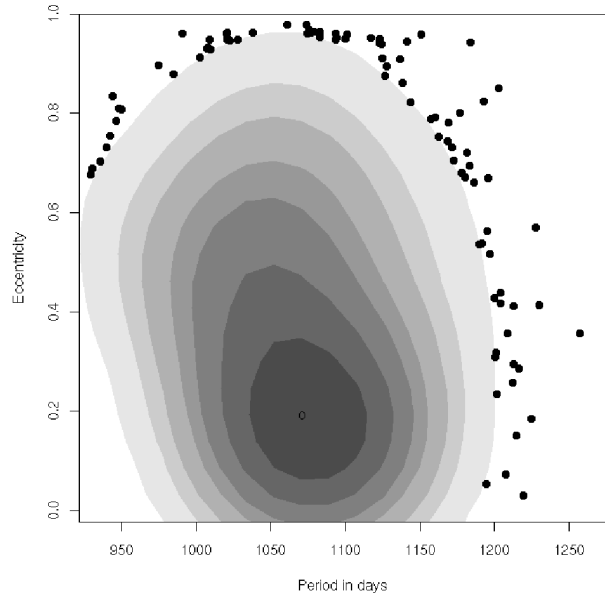


Figure 7. The joint posterior distribution of orbital period T and eccentricity e for the companion to HD 187085. The contours represent probability coverage=0.01,0.05,0.1,0.2,0.3,0.4,0.5 and 0.7. The circle in the centre represent the mode of the joint probability distribution. The dots outside the contour show the samples that fall outside 99% coverage probability.

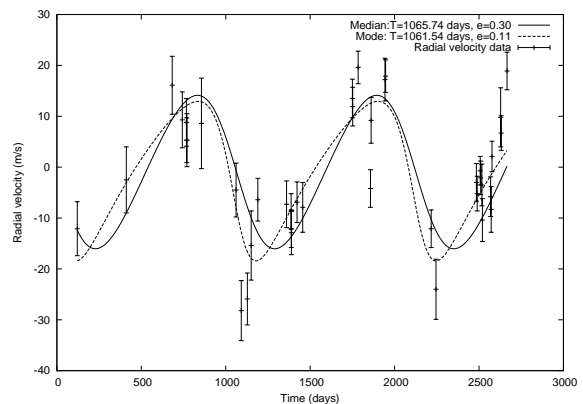


Figure 8. Possible orbital solutions for the companion to HD187085.

statistic. Table 8 shows the median of samples from *ExoFit* and the Keplerian orbit obtained is plotted in Fig. 10 along with the observed data and uncertainties. Table 7 shows the sensitivity to changing the priors to Top Hat. We note that the ‘noise’ factor s is 10 times larger than the measurement errors, probably indicating the presence of an unaccounted signal in the radial velocity data.

7 DISCUSSION

We present a new software package, *ExoFit*, for estimating the orbital parameters from radial velocity data in a Bayesian framework by utilising Markov Chain Monte Carlo

Table 6. A comparison of estimators for orbital parameters of the companion to HD 187085. The columns provide the posterior mean (and standard deviation), median (and 25% and 75% quantiles) and the maximum a posteriori, i.e. posterior mode (and 68.3% credible regions). The last column is from the published results of Jones et al. (errors were not provided in their paper). Here $m_p \sin i$ and a are calculated by assuming the mass of the star $m_s = 1.16 M_\odot$.

Parameter	<i>ExoFit</i>	<i>ExoFit</i>	<i>ExoFit</i>	Jones et al
	Mean	Median	Mode	
$T(\text{days})$	1065.84 ± 45.75	$1065.74_{-30.26}^{+30.48}$	$1061.54_{41.43}^{+51.53}$	986
$K(\text{ms}^{-1})$	16.55 ± 4.49	$15.67_{-1.49}^{+1.93}$	$15.08_{-2.28}^{+2.73}$	17
$V(\text{ms}^{-1})$	-0.94 ± 1.56	$-0.93_{-1.02}^{+1.00}$	$-0.81_{-1.64}^{+1.38}$	
e	0.33 ± 0.22	$0.30_{-0.15}^{+0.20}$	$0.11_{-0.10}^{+0.29}$	0.47
ϖ	118.57 ± 23.19	$112.39_{-11.85}^{+18.58}$	$95.32_{-5.15}^{+29.22}$	94
χ	0.11 ± 0.06	$0.11_{-0.04}^{+0.04}$	$0.10_{-0.06}^{+0.07}$	
s	5.47 ± 1.08	$5.40_{-0.68}^{+0.72}$	$5.21_{-0.95}^{+1.15}$	
T_p (JD -2450000)	993 ± 60.49	992_{-32}^{+30}	$998.43_{-64.29}^{+44.47}$	912
$m_p \sin i (M_{Jup})$	0.81 ± 0.10	$0.81_{-0.07}^{+0.06}$	$0.82_{-0.12}^{+0.08}$	0.75
$a(\text{AU})$	2.14 ± 0.06	$2.14_{-0.04}^{+0.04}$	$2.14_{-0.06}^{+0.06}$	2.05

Table 7. Mean and standard deviation of posterior modes of parameters obtained from 10 trial runs of *ExoFit*.

	HD 187085	HD 187085	HD159868	HD159868
Parameter	Gregory's	Top Hat	Gregory's	Top Hat
T (days)	1068.49 ± 3.94	1068.57 ± 2.36	998.04 ± 4.88	1007.38 ± 5.23
K (ms^{-1})	15.35 ± 0.30	16.34 ± 0.66	43.16 ± 4.93	41.44 ± 2.00
V (ms^{-1})	-1.03 ± 0.10	-0.99 ± 0.12	1.13 ± 0.21	1.05 ± 0.28
e	0.14 ± 0.03	0.16 ± 0.51	0.70 ± 0.04	0.68 ± 0.02
ϖ	96.30 ± 2.86	96.87 ± 2.29	94.05 ± 4.28	98.50 ± 3.28
χ	0.11 ± 0.004	0.11 ± 0.05	0.68 ± 0.002	0.68 ± 0.001
s (ms^{-1})	5.28 ± 0.07	5.03 ± 0.06	9.52 ± 0.10	9.77 ± 0.15
T_p (JD -2450000)	992.96 ± 0.42	993.74 ± 0.05	706.15 ± 2.77	689.35 ± 1.76
$m_p \sin i (M_{Jup})$	0.80 ± 0.006	0.81 ± 0.008	1.61 ± 0.03	1.60 ± 0.01
a (AU)	2.14 ± 0.005	2.14 ± 0.003	2.01 ± 0.006	2.02 ± 0.006

(MCMC) simulations with the Metropolis-Hastings algorithm. *ExoFit* can search for one or two planets in a given radial velocity data and can easily be extended to search for more planets. We applied *ExoFit* to simulated data sets to check the accuracy of the parameters extracted. As an illustration we re-analysed the orbital solution of companions to HD 187085 and HD 159868 from the published radial velocity data. We confirm the degeneracy reported for orbital parameters of the companion to HD 187085 and show that a low eccentricity orbit is more probable for this planet. For HD 159868 we obtained slightly different orbital solution and a relatively high ‘noise’ factor indicating the presence of an unaccounted signal in the radial velocity data. We have also studied the sensitivity of the results to changes in the Bayesian priors. We plan to extend *ExoFit* to search for

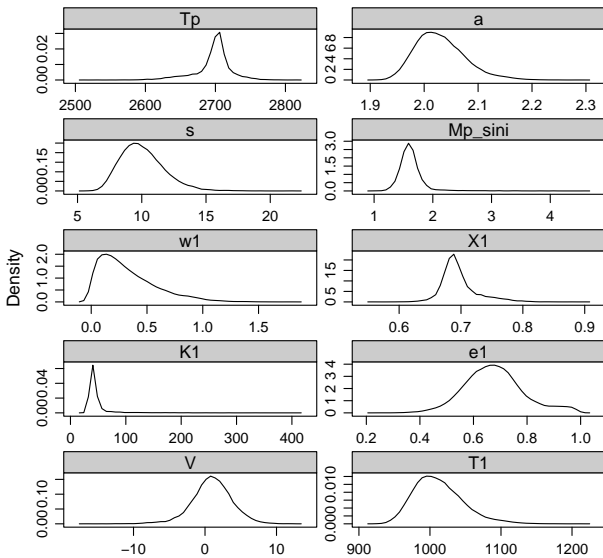
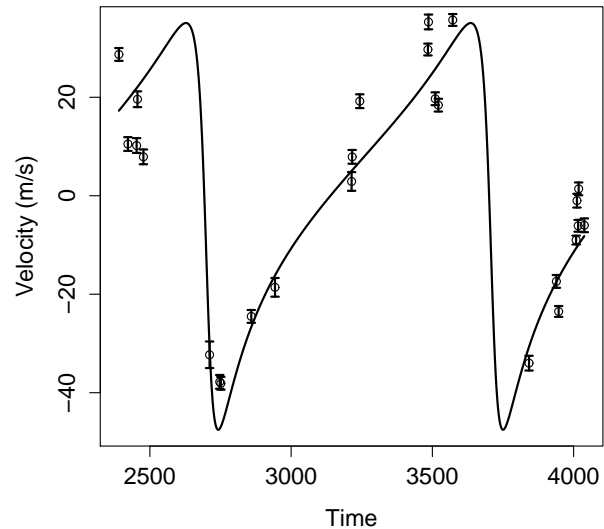
more than two planets and to analyse transit photometry data.

8 ACKNOWLEDGEMENTS

We are grateful to Jean-Philippe Beaulieu, Farah Islam, David Kipping, Yasushi Suto and Giovanna Tinetti for helpful discussions. SB acknowledges a Royal Astronomical Society studentship grant and OL acknowledges a Royal Society Wolfson Research Merit Award.

Table 8. A comparison of the orbital parameters of the companion to HD 159868 from *ExoFit* and the published results of O’Toole et al. (2007). Here $m_p \sin i$ and a are calculated by assuming the mass of the star $m_s = 1.09 M_\odot$.

Parameter	<i>ExoFit</i>	<i>ExoFit</i>	<i>ExoFit</i>	O’Toole et al
	Mean	Median	Mode	
T (days)	1012.28 ± 34.53	$1008.25^{+24.6}_{-20.71}$	$997.05^{+40.45}_{-24.41}$	986 ± 9
K (ms^{-1})	46.87 ± 25.63	$41.30^{+5.17}_{-3.93}$	$40.34^{+6.67}_{-6.6}$	43.3 ± 2
V (ms^{-1})	0.96 ± 2.80	$1.00^{+1.77}_{-1.64}$	$0.89^{+2.71}_{-2.37}$	
e	0.67 ± 0.11	$0.67^{+0.06}_{-0.07}$	$0.67^{+0.09}_{-0.11}$	0.69 ± 0.02
ϖ	108.33 ± 14.32	$105.11^{+11.4}_{-7.44}$	$96.81^{+16.10}_{-16.44}$	97 ± 3
χ	0.69 ± 0.02	$0.69^{+0.01}_{-0.02}$	$0.68^{+0.02}_{-0.02}$	–
s (ms^{-1})	10.06 ± 1.69	$9.86^{+1.18}_{-1.01}$	$9.49^{+1.71}_{-1.41}$	–
T_p (JD -2450000)	672.44 ± 26.5	684.89^{+9}_{-11}	$710.80^{+14.35}_{-20.74}$	700 ± 9
$m_p \sin i$ (M_{Jup})	1.62 ± 0.23	$1.59^{+0.09}_{-0.09}$	$1.59^{+0.15}_{-0.14}$	1.7 ± 0.3
a (AU)	2.03 ± 0.04	$2.02^{+0.03}_{-0.028}$	$2.01^{+0.05}_{-0.04}$	2 ± 0.3

**Figure 9.** Posterior distribution of orbital parameters of the companion to HD 159868.**Figure 10.** Best fit Keplerian orbit for the companion to HD 159868.

REFERENCES

- Bayes T., 1763, Philosophical Transactions of the Royal Society, 53, 370
- Berg B. A., 2004, Markov Chain Monte Carlo Simulations And Their Statistical Analysis: With Web-based Fortran Code. World Scientific
- Berger J. O., 1980, Statistical Decision Theory and Bayesian Analysis, 2 edn. Springer-Verlag New York Inc, 175 Fifth Avenue, New York, NY10010, USA
- Bouchy F., Bazot M., Santos N. C., 2005, A&A, 440, 609
- Butler et al R. P., 2006, ApJ, 646, 505
- Cumming A., 2004, MNRAS, 354, 1165
- Cumming A., Marcy G. W., Butler R. P., 1999, ApJ, 526, 890
- Ford E. B., 2005, AJ, 129, 1706
- Ford E. B., 2006, ApJ, 642, 505
- Ford E. B., Gregory P. C., 2007, Statistical Challenges in Modern Astronomy IV, ASP Conference Series, 371, 189
- Gilks W. R., Richardson S., Spiegelhalter D. J., eds, 1996, Markov Chain Monte Carlo in Practice. Chapman & Hall London
- Graves T. L., 2007, Journal of Computational & Graphical Statistics, 16, 24
- Gregory P. C., 2005a, ApJ, 631, 1198

- Gregory P. C., 2005b, Bayesian Logical Data Analysis for the Physical sciences: A comparative Approach with “Mathematica” Support. Cambridge: Cambridge University Press
- Haario H., Saksman E., Tamminen J., 1999, Computational Statistics, 14, 375
- Hastings W. K., 1970, Biometrika, 57, 97
- Hyndman R. J., 1996, The American Statistician, 50, 120
- Jones H. R. A., Butler R. P., Tinney C. G., Marcy G. W., Carter B. D., Penny A. J., McCarthy C., Bailey J., 2006, MNRAS, 369, 249
- Levenberg K., 1944, Quarterly of Applied Mathematics, 2, 164
- Lewis A., Bridle S., 2002, Phys. Rev. D, 66, 103511
- Lomb N. R., 1976, Ap&SS, 39, 447
- Marquardt D., 1963., SIAM Journal on Applied Mathematics, 11, 431
- Mayor M., Pepe F., Queloz D., Bouchy F., Rupprecht G., Lo Curto G., Avila G., Benz W., Bertaux J.-L., Bonfils X., Dall T., Dekker H., 2003, The Messenger, 114, 20
- Metropolis N., Rosenbluth A. W., Rosenbluth M. N., H. T. A., Teller E., 1953, Journal of Chemical Physics, 21, 1087
- Murray C. D., Dermott S. F., 2000, Solar System Dynamics. Cambridge University Press
- O’Hagan A., Forster J., 2004, Bayesian Inference, 2 edn. Vol. 2B of Kendall’s Advanced Theory of Statistics, Oxford University Press Inc, 198 Madison Avenue, New York, NY10016
- Ohta Y., Taruya A., Suto Y., 2005, ApJ, 622
- O’Toole S. J., Butler R. P., Tinney C. G., Jones H. R. A., Marcy G. W., Carter B., McCarthy C., Bailey J., Penny A. J., Apps K., Fischer D., 2007, ApJ, 660, 1636
- Pepe F., Mayor M., Queloz et al D., 2004, A&A, 423, 385
- Scargle J. D., 1982, ApJ, 263, 835